

Spin wave dispersion based on the quasiparticle self-consistent *GW* method: NiO, MnO and α -MnAs

Takao Kotani and Mark van Schilfgaarde

School of Materials, Arizona State University, Tempe, Arizona, 85287-6006, USA

(Dated: October 24, 2018)

Abstract

We present spin wave dispersions for MnO, NiO, and α -MnAs based on the recently-developed quasiparticle self-consistent *GW* method (QSGW), which determines an optimum quasiparticle picture. For MnO and NiO, QSGW results are in rather good agreement with experiments, in contrast to the LDA and LDA+*U* descriptions. For α -MnAs, we find a collinear ferromagnetic ground state in QSGW, while this phase is unstable in the LDA.

PACS numbers: 71.15-m, 71.10-w, 71.20-Eh

I. INTRODUCTION

The magnetic linear response is a fundamental property of solids. It is given by the spin susceptibility when the spin-orbit coupling is neglected (as we will do in this article). The spin susceptibility is equivalent with the spin fluctuations, as can be seen from the fluctuation-dissipation theorem. Low-energy spin fluctuations can control some low energy phenomena such as magnetic phase transitions, and contribute to resistivity through spin-flip scattering of electrons. Antiferro(AF)-magnetic spin-fluctuations can play an important role in high- T_c superconductors^{1,2}. It is also the central quantity entering into the description of quantum-critical phenomena^{3,4}. We expect that reliable first-principle methods to calculate the spin susceptibility should give important clues to understand these phenomena. In this paper, we concentrate on the magnetically-ordered systems, where the spin susceptibility should be dominated by spin waves (SW) at low energy.

In spite of the recent development of such methods, we still have large class of systems where we can hardly calculate the spin susceptibility, e.g, as discussed in Ref.5. A typical example is MnO; Solovyev and Terakura gave an analysis for the calculation of its SW energies⁶. Then they showed main problem is in the non-interacting one-body Hamiltonian H^0 from which we calculate the non-interacting spin susceptibility used for the calculation of the SW energies. H^0 given by the local density approximation (LDA), LDA+ U , or even the optimized effective potential (OEP)⁷ are not adequate. In the LDA+ U case, they traced the error to a misalignment of the O($2p$) bands relative to the Mn($3d$) bands. It is impossible to choose the U parameter to correct the misalignment, because the U parameter can only control the exchange splitting within $3d$ bands. A possibility may be adding some other parameter in addition to U so as to correct the misalignment; however, such a procedure including more parameters become less universal. This situation is somehow similar with the case of optical response (dielectric function) calculation for semiconductors, where H^0 given by LDA is with too small band gap, thus requires some additional correction like scissors operator. Our case for the spin susceptibility for MnO is rather worse; LDA supplies too problematic H^0 to be corrected in a simple manner.

Another possibility is to obtain H^0 by some hybrid functional; it has been shown that it can work as explained below, however, it could be problematic from the view of universality. Muscat, Wander, and Harrison claimed that a functional B3LYP^{8,9} (containing 20% of Fock

exchange) works even for solids. However, Franchini, Bayer, Podloucky, Paier and Kresse¹⁰ showed that a little different functional, PBE0 is better than B3LYP in order to obtain better agreement with experiments as for the exchange interaction. PBE0 is a combination of 25% of the Fock exchange with a generalized-gradient approximation(GGA)¹¹. However, such a functional could be not so universal, mainly because the effect of screening (therefore the ratio of the Fock exchange) are dependent on materials. In fact, de P. R. Moreira, Illas, and Martin¹² reported that a hybrid functional containing 35% of Fock exchange gives best results for NiO; the ratio of the Fock exchange is rather different from the case of MnO by Franchini et al. This is somehow consistent with latest careful examinations by Fuchs Furthmuller, Bechstedt, Shishkin and Kresse¹³ and Paier, Marsman, and Kresse¹⁴; they clarify the fact that a hybrid functional should be limited, because the screening effects (corresponding to the ratio of the Fock exchange) can be material-dependent. These seem to indicate a difficulty to pick up an universally-applicable hybrid functional. This difficulty becomes more problematic when we treat inhomogeneous systems, e.g, to treat the Schotkey-barrier problem, where the screening effects are very different in metal side and in semiconductor side.

Considering these facts, it is necessary to start from good H^0 without such problems. Our recently-developed quasiparticle self-consistent GW method (QSGW), which includes the above screened exchange effects in a satisfactory manner^{15,16,17,18,19,20,21}. QSGW determines a reference system of H^0 representing optimum quasiparticle (QP) picture in the sense of Landau-Silin Fermi liquid theory. As discussed in Ref.19, it is based on a self-consistent perturbation theory within all-electron full-potential GW approximation (GWA), but it is conceptually very different from the usual full self-consistent GW . QSGW self-consistently determines not only H^0 , but also the screened interaction W , and the Green's function G simultaneously.

We have shown that QSGW gives QP energies, spin moments, dielectric functions and so on in good agreement with experiments for wide range of materials. There are systematic but a little disagreement from experiments. For example, as shown in Fig.1 in Ref.17, we see error that calculated band gaps are systematically larger than those by experiments. A recent development by Shishkin, Marsman and Kresse²¹ confirmed our conjecture¹⁷ that the inclusion of electron-hole correlation effect in W will correct the error. Their method is a simplified version of the full Bethe-Salpeter equation (BSE) for W ; it includes only the

static and spatially-local part of the first-order term in the BSE, based on the procedure given by Sottile, Olevano, and Reining²². However, since the band-gap error itself is small enough, such simplifications may cause no problem. Considering this success, we believe that QSGW is a basis for future development of the electronic structure calculations.

In this paper, we treat MnO and NiO with AF ordering II (AF-II)²³, and α -MnAs. α -MnAs is NiAs-type grown on GaAs epitaxially, thus is a candidate for spintronics applications²⁴. For this purpose, we have developed a procedure to calculate the spin susceptibility at zero temperature. It is a general procedure for a given self-consistent method which determines H^0 , even when H^0 contains non-local potentials as in the Hartree-Fock method. We then apply it to LDA, and to QSGW. After we explain the method in the next section, we will show SW energies obtained with QSGW are in good agreement with experiments for MnO and NiO. See Ref.19 for dielectric functions for NiO and MnO. For MnAs, our calculation shows that a collinear FM ground state is stable in QSGW though it does not in LDA.

At the end of introduction, we give a discussion to justify using the one-particle picture (band picture) of “Mott insulator” for MnO and NiO; it is essentially given by Terakura, Williams, Oguchi, and Kübler in 1984²³ (in the following discussion, “charge transfer type” or “Mott type” does not matter). Based on the one-particle picture, the existence of some spin moment (or exchange splitting, equivalently) at each cation site is very essential to make the system insulator. This is consistent with the experimental facts that all the established “Mott insulator” are accompanied with the AF (or some) magnetic ordering. Thus the concept “Mott insulator vs Band insulator” often referred to is misleading, or rather confusing. In order to keep the system insulating, any ordering of spin moment is possible provided the system retains a sufficiently large enough exchange splitting at each site (we need to use the non-collinear mean-field method). In this picture, metal-insulator transition at zero-temperature (e.g, consider a case to compress NiO) is nothing but the first-order transition from magnetic-phase to the non-magnetic phase described by a band picture. On the other hand, the transition at finite temperature to para-magnetic phase occurs because of the entropy effects due to the accumulation of SWs; then the transition is not accompanied with the metal-insulator transition because the exchange splitting (or local moment) at each site is kept even above the Néel temperature T_N . This picture is very different from that assumed in Refs.5,25, where they emphasize the priority of their

method LDA + U + “dynamical mean field theory (DMFT)”. On the contrary to their claim, we insist that our treatment should be prior and much closer to reality for such systems, because of the following reasons.

i) One-particle treatment in our QSGW allows us to perform parameter-free accurate calculations where we treat all the electrons on the same footing; this is very critical because of the relative position of cation $3d$ bands to $O(2p)$ is important (also their hybridization; we have no SW dispersion without hybridization). Further, we are free from uncontrollable double-counting problem²⁶, nor the parameter like U which is externally introduced by hand. In contrast, LDA+ U +DMFT carries these same problems which are in LDA+ U , or rather highly tangled. Thus it is better to take a calculation by LDA+ U +DMFT as a model in cases. As an example, we guess that the distribution probability of the number of $5f$ electrons in δ -Plutonium calculated by LDA+ U +DMFT²⁷ will be easily changed if we shift the relative position (and hybridization) of $5f$ band with respect to other bands.

ii) The DMFT at zero temperature takes into account the quantum-mechanical onsite fluctuation which is not included within the one-particle picture; it allows a system to be an insulator without magnetic order. However, we expect that such quantum-mechanical fluctuation is not essentially important to determine its ground state for materials like NiO and MnO. This is based on our findings that QSGW results can well reproduce the optical response^{15,19}, and also the magnetic responses as shown in this paper. These QSGW results are not perfect, however, supplies us a good enough starting point. For example, in order to describe the d-d multiplet intra transitions (e.g, see Fig.6 of Ref.28 by Fujimori and Minami; they are very weak in comparison with interband transitions), it may be easier to start from the cluster models or so; however, parameters used in these models will be determined by QSGW even in such a case.

iii) At finite temperature, the DMFT can take into account not only such quantum-mechanical fluctuations, but also the onsite thermal fluctuations simultaneously; this is an advantage of DMFT. However, in MnO and NiO, low-energy primary fluctuations are limited to the transverse spin fluctuations except

phonons. These can be included in DMFT but it is essentially described by the local-moment-disorder²⁹ as the thermal average of the one-particle picture. Thus no advantage of DMFT if only the thermal fluctuations are important.

II. METHOD FOR SPIN SUSCEPTIBILITY CALCULATION

We may divide first-principle methods to calculate SW energies into three classes; (A), (B), and (C). (A) is from the Heisenberg Hamiltonian, whose exchange parameters J are determined from the total energy differences of a set of different spin configurations^{30,31,32}. (B) and (C) are based on perturbation. (B) estimates J from static infinitesimal spin rotations^{33,34}. We go through the Heisenberg model even in (B). In contrast, (C) determines SW energies directly from the poles in the transverse spin susceptibility $\chi^{+-}(\mathbf{r}, \mathbf{r}', t - t')$ (defined below) in the random phase approximation (RPA) or time-dependent LDA (TDLDA)^{35,36,37}. (C) gives the spectrum including life time, and spin-flip excitations. Because (C) is technically difficult, (A) or (B) have been mainly used. (B) is regarded as a simplification of (C); but real implementations entail further approximations.

Our method belongs to (C). Our formalism is applicable to any H^0 even if it contains non-local potential. At the beginning, we introduce some notations to treat the time-ordered transverse spin susceptibility

$$\chi^{+-}(\mathbf{r}, \mathbf{r}', t - t') = -i\langle T(\hat{S}^+(\mathbf{r}, t)\hat{S}^-(\mathbf{r}', t')) \rangle. \quad (1)$$

$\langle \dots \rangle$ denotes the expectation value for the ground state; $T(\dots)$ means time-ordering, and $\hat{S}^\pm(\mathbf{r}, t) = \hat{S}^x(\mathbf{r}, t) \pm i\hat{S}^y(\mathbf{r}, t)$ are the Heisenberg operators of spin density. Since we assume collinear magnetic ordering for the ground state, we have $\langle \hat{S}^x(\mathbf{r}, t) \rangle = \langle \hat{S}^y(\mathbf{r}, t) \rangle = 0$; $2\langle \hat{S}^z(\mathbf{r}, t) \rangle = M(\mathbf{r}) = n^\uparrow(\mathbf{r}) - n^\downarrow(\mathbf{r})$. $n^\uparrow(\mathbf{r})$ and $n^\downarrow(\mathbf{r})$ mean up and down electron densities. $M_a(\mathbf{r})$ is the component of $M(\mathbf{r})$ on the the magnetic sites a in unit cell. The Fourier transform of χ^{+-} is

$$\chi^{+-}(\mathbf{T} + \mathbf{r}, \mathbf{r}', \omega) = \frac{1}{N} \sum_{\mathbf{q}} e^{i\mathbf{q}\mathbf{T}} \chi_{\mathbf{q}}^{+-}(\mathbf{r}, \mathbf{r}', \omega), \quad (2)$$

where \mathbf{T} is a lattice translation vector, and N the number of sites. \mathbf{r}, \mathbf{r}' are limited to a unit cell.

Next we derive two conditions Eq. (4) and Eq. (5) below, which χ^{+-} rigorously satisfies. Taking the time derivative of Eq. (1), we obtain

$$\begin{aligned} & \frac{\partial}{\partial t'} \int d^3 r' \chi^{+-}(\mathbf{r}', \mathbf{r}, t' - t) \\ &= \int d^3 r' \langle T([\hat{H}, \hat{S}^+(\mathbf{r}', t')], \hat{S}^-(\mathbf{r}, t)] \rangle - i \int d^3 r' \langle [\hat{S}^+(\mathbf{r}', t'), \hat{S}^-(\mathbf{r}, t)] \rangle \delta(t' - t), \end{aligned} \quad (3)$$

where $[A, B] = AB - BA$. \hat{H} denotes the total Hamiltonian of the system. We have used $\frac{\partial \hat{S}^+(\mathbf{r}', t')}{\partial t'} = i[\hat{H}, \hat{S}^+(\mathbf{r}', t')]$. We assume \hat{H} has rotational symmetry in spin space, so that $[\hat{H}, \int d^3 r' \hat{S}^+(\mathbf{r}', t')] = 0$. Then the first term in the right-hand side is zero. The second term reduces to $M(\mathbf{r})$ because $[\hat{S}^+(\mathbf{r}', t), \hat{S}^-(\mathbf{r}, t)] = 2\hat{S}^z(\mathbf{r}, t)\delta(\mathbf{r} - \mathbf{r}')$. Thus Eq. (3) is reduced to be

$$\int_{\Omega} d^3 r' \chi_{\mathbf{q}=0}^{+-}(\mathbf{r}', \mathbf{r}, \omega) = \frac{M(\mathbf{r})}{\omega}, \quad (4)$$

where Ω denotes the unit-cell volume. Note that Eq. (4) is satisfied for any ω . At $\omega \rightarrow 0$, this means that $M(\mathbf{r})$ is the eigenfunction of $\chi_{\mathbf{q}=0}^{+-}(\mathbf{r}, \mathbf{r}', \omega)$ with divergent eigenvalue; this is because a magnetic ground state is degenerate for homogeneous spin rotation. Another condition is the asymptotic behavior as $\omega \rightarrow \infty$. It is given as

$$\chi^{+-}(\mathbf{r}', \mathbf{r}, \omega) \rightarrow \frac{M(\mathbf{r})}{\omega} \delta(\mathbf{r} - \mathbf{r}') + O(1/\omega^2). \quad (5)$$

This can be easily derived from the spectrum representation of χ^{+-} . We use Eq. (4) and Eq. (5) to determine the effective interaction \bar{U} in the following.

As in Ref. 38, we define the effective interaction $U(\mathbf{r}, \mathbf{r}', \omega)$ as the difference between $(\chi^{+-})^{-1}$ and the non-interacting counterpart: $(\chi^{0+-})^{-1}(\mathbf{r}, \mathbf{r}', \omega)$;

$$(\chi^{+-})^{-1} = (\chi^{0+-})^{-1} + U. \quad (6)$$

In TDLDA, U is the second derivative of the exchange-correlation energy, $U(\mathbf{r}, \mathbf{r}') = -\delta^2 E_{xc} / \delta S^+(\mathbf{r}) \delta S^-(\mathbf{r}') = I_{xc}(\mathbf{r}) \delta(\mathbf{r} - \mathbf{r}')$, which is local $U(\mathbf{r}, \mathbf{r}') \propto \delta(\mathbf{r} - \mathbf{r}')$, ω -independent, and positive. Then we can show that χ^{+-} in TDLDA satisfies conditions Eq. (4) and Eq. (5) automatically³⁹. In the case of H^0 containing nonlocal potentials (e.g. in the case of the Hartree-Fock method), U is no longer independent of ω . This is because the natural expansion of χ^{+-} in the many-body perturbation theory requires solving the Bethe-Salpeter Eq. for the two-body propagator $\chi^{+-}(\mathbf{r}_1, \mathbf{r}_2; \mathbf{r}_3, \mathbf{r}_4, \omega)$, thus U defined in Eq. (6) is not directly identified as a kinds of diagrams. Ref.37 did not pay attention to this point. We can

calculate χ^{0+-} in Eq. (6) as

$$\begin{aligned}\chi_{\mathbf{q}}^{0+-}(\mathbf{r}, \mathbf{r}', \omega) &= \sum_{\mathbf{k}\downarrow}^{\text{occ}} \sum_{\mathbf{k}'\uparrow}^{\text{unocc}} \frac{\Psi_{\mathbf{k}\downarrow}^*(\mathbf{r}) \Psi_{\mathbf{k}'\uparrow}(\mathbf{r}) \Psi_{\mathbf{k}'\uparrow}^*(\mathbf{r}') \Psi_{\mathbf{k}\downarrow}(\mathbf{r}')}{\omega - (\epsilon_{\mathbf{k}'\uparrow} - \epsilon_{\mathbf{k}\downarrow}) + i\delta} \\ &+ \sum_{\mathbf{k}\downarrow}^{\text{unocc}} \sum_{\mathbf{k}'\uparrow}^{\text{occ}} \frac{\Psi_{\mathbf{k}\downarrow}^*(\mathbf{r}) \Psi_{\mathbf{k}'\uparrow}(\mathbf{r}) \Psi_{\mathbf{k}'\uparrow}^*(\mathbf{r}') \Psi_{\mathbf{k}\downarrow}(\mathbf{r}')}{-\omega - (\epsilon_{\mathbf{k}\downarrow} - \epsilon_{\mathbf{k}'\uparrow}) + i\delta},\end{aligned}\quad (7)$$

where $\mathbf{k}' = \mathbf{q} + \mathbf{k}$. $\chi^{0+-}(\mathbf{r}, \mathbf{r}', \omega = 0)$ is negative definite matrix. Our definition of χ^{+-} and also χ^{0+-} can be different in sign from other definitions in the literature because we start from Eq. (1).

In order to realize an efficient computational method, we assume that the magnetization is confined to magnetic atomic sites, and we explicitly treat only a degree of freedom of spin rotation per each site. Then we can determine U with the help of Eq. (4) and Eq. (5) as in the following. As a choice to extract the degrees of freedom, we consider a matrix $D(\mathbf{q}, \omega)$ as

$$(D(\mathbf{q}, \omega))_{aa'} = \int_a d^3r \int_{a'} d^3r' \bar{e}_a(\mathbf{r}) \chi_{\mathbf{q}}^{+-}(\mathbf{r}, \mathbf{r}', \omega) \bar{e}_{a'}(\mathbf{r}'), \quad (8)$$

and $D^0(\mathbf{q}, \omega)$ defined in the same manner. The dimension of the matrix $D(\mathbf{q}, \omega)$ is the number of magnetic sites. Here we define $e_a(\mathbf{r}) = M_a(\mathbf{r})/M_a$ where $M_a = \int_a d^3r M_a(\mathbf{r})$; and define $\bar{e}_a(\mathbf{r})$ so that $\bar{e}_a(\mathbf{r}) \propto e_a(\mathbf{r})$ and $\int d^3r \bar{e}_a(\mathbf{r}) e_a(\mathbf{r}) = 1$; thus $\bar{e}_a(\mathbf{r}) = e_a(\mathbf{r}) / \int_a d^3r (e_a(\mathbf{r}))^2$. Corresponding to Eq. (6), we define the effective interaction $(\bar{U}(\mathbf{q}, \omega))_{aa'}$ as

$$(D(\mathbf{q}, \omega))^{-1} = (D^0(\mathbf{q}, \omega))^{-1} + \bar{U}(\mathbf{q}, \omega). \quad (9)$$

For the calculation of $D^0(\mathbf{q}, \omega)$ from Eq. (7), we use the tetrahedron technique¹⁹, which allow us to use fewer \mathbf{k} points in the first Brillouin zone (BZ) than those required for the sampling method³⁷. \bar{U} defined in Eq. (9) should include all the downfolded contributions from all the other degrees of freedom. We now assume that \bar{U} is \mathbf{q} -independent and site-diagonal, so that it can be written as $\bar{U}_{aa'}(\mathbf{q}, \omega) = U_a(\omega) \delta_{aa'}$. Since Eq. (4) reduces to a constraint $\sum_{a'} (D(\mathbf{q} = 0, \omega))_{a'a} = M_a/\omega$, we determine $\bar{U}_a(\omega)$ from

$$\bar{U}_a(\omega) = \frac{\omega}{M_a} \delta_{aa'} - \left(\frac{\sum_b M_b (D^0(\mathbf{q} = 0, \omega))_{ba}^{-1}}{M_a} \right) \delta_{aa'}.$$

With this $\bar{U}_a(\omega)$ for Eq. (9), we finally have

$$(D(\mathbf{q}, \omega))^{-1} = \frac{\omega}{M_a} \delta_{aa'} - \bar{J}(\mathbf{q}, \omega), \quad (10)$$

$$\bar{J}(\mathbf{q}, \omega) = - (D^0(\mathbf{q}, \omega))^{-1} + \left(\frac{\sum_b M_b (D^0(\mathbf{q} = 0, \omega))_{ba}^{-1}}{M_a} \right) \delta_{aa'}. \quad (11)$$

Eq. (5) reduces to $(D(\mathbf{q}, \omega))_{a'a}^{-1} \rightarrow \frac{\omega}{M_a} \delta_{aa'}$ at $\omega \rightarrow \infty$; $(D(\mathbf{q}, \omega))_{a'a}^{-1}$ given by Eq. (10) gives this correct asymptotic behavior. Note that we determine U just from the requirement Eq. (4) because of our approximations “onsite only U ” and “a basis per magnetic site”. If we need to go beyond such approximation (e.g. multiple basis per site), it will be necessary to introduce additional informations, e.g. a part of $\chi(\mathbf{q}, \omega = 0)$ evaluated by numerical linear-response calculations (perform the QSGW self-consistent calculations with bias fields). By Fourier transformation, we can transform $(D(\mathbf{q}, \omega))_{a'a}$ into $D_{RR'}(\omega)$; the same is also for D^0, J and so on. Here $R = \mathbf{T}a$ is the composite index to specify an atom in the crystal. For later discussion we define

$$J(\mathbf{q}, \omega) = -(D^0(\mathbf{q}, \omega))^{-1} + \frac{\delta_{aa'}}{D_{aa}^0(\omega)}, \quad (12)$$

where $D_{aa}^0(\omega)$ is shorthand for $D_{\mathbf{T}a\mathbf{T}a}^0(\omega)$; it is \mathbf{T} independent. The second term in Eq. (12) is included just in order to remove the onsite term from J . Then Eq. (11) can be written as

$$\bar{J}(\mathbf{q}, \omega) = J(\mathbf{q}, \omega) - \left(\frac{\sum_b M_b J_{ba}(\mathbf{q} = 0, \omega)}{M_a} \right) \delta_{aa'}. \quad (13)$$

Here, the second term (onsite term) in Eq. (12) is irrelevant because of the cancellation between two terms in Eq. (13).

The preceding development for $(D(\mathbf{q}, \omega))^{-1}$ facilitates a comparison with the Heisenberg model, whose Hamiltonian is $\mathcal{H} = -\sum_R \sum_{R'} J_{RR'}^{\mathcal{H}} \mathbf{S}_R \cdot \mathbf{S}_{R'}$ ($R = \mathbf{T}a$). As shown in Appendix A, the inverse of the susceptibility in the Heisenberg model is:

$$(D^{\mathcal{H}}(\mathbf{q}, \omega))^{-1} = \frac{\omega}{M_a} \delta_{aa'} - \bar{J}^{\mathcal{H}}(\mathbf{q}), \quad (14)$$

where $M_a = |2\mathbf{S}_R|$. Let us compare Eq. (14) with Eq. (10). This $\bar{J}_{aa'}^{\mathcal{H}}(\mathbf{q})$ is given by Eq. (A9), which is almost the same as Eq. (13); only the difference is whether we use $J^{\mathcal{H}}$ or J . This suggests how to construct the Heisenberg model which reproduces Eq. (10) as good as possible; a possibility is that we simply assign $J(\mathbf{q}, \omega = 0)$ (neglecting the ω -dependence) as $J^{\mathcal{H}}(\mathbf{q})$. We have confirmed that this approximation is good enough to reproduce SW energies in the case for MnO and NiO. However, it is not true in the case of α -MnAs; then we have used another procedure given by Katsnelson and Lichtenstein³⁹: we identify $J(\mathbf{q}, \omega = (\text{SW energy at } \mathbf{q}))$ as $J^{\mathcal{H}}$. This construction exactly reproduces SW energies calculated from $D^{\mathbf{q}, \omega}$.

As a further approximation to calculate $J(\mathbf{q}, \omega = 0)$, we can expand it in real space as (omit ω for simplicity)

$$-J_{RR'} = (D_{RR'}^0)^{-1} - \frac{\delta_{RR'}}{D_R^0} = (D_R^0 \delta_{RR'} + D_{RR'}^{0,\text{off}})^{-1} - \frac{\delta_{RR'}}{D_R^0} \approx \frac{1}{D_R^0} D_{RR'}^{0,\text{off}} \frac{1}{D_{R'}^0}, \quad (15)$$

where we use Eq. (12); we use notation that onsite part $D_R^0 = D_{RR}^0$ and the off-site part $D_{RR'}^{0,\text{off}} = D_{RR'}^0 - D_{RR'}^0 \delta_{RR'}$. Here we have used the assumption that $D_{RR'}^{0,\text{off}}$ are small in comparison with onsite term D_R^0 . This approximation corresponds to the usual second-order perturbation scheme of the total energy; if the spin rotation perfectly follows the rotation of the one-particle potential, $\frac{1}{D_R^0}$ is trivial; it is equal to the difference of the one-particle potential between spins (exchange-correlation potential in the case of DF) because $\frac{1}{D_R^0}$ is the inverse linear-response to determine the one-particle potential for given spin rotation. Essentially the same equation as Eq. (15) was used in Refs. 33,34. In cases, this approximation is somehow mixed up with the “long wave approximation” to expanding J around $D^0(\mathbf{q} = 0)^{38}$; however, they should be differentiated. In order to have rough estimate of $J_{RR'}$, we can further reduce this to the two sites model as originally presented by Anderson and Hasegawa^{40,41}. For an AF magnetic pair (half-filled case), we obtain the following estimate:

$$J_{RR'} \approx -\frac{1}{D_R} D_{RR'}^{0,\text{off}} \frac{1}{D_{R'}} \sim -\frac{4t^2}{\Delta E_{\text{ex}} M}, \quad (16)$$

where t denotes the transfer integral, and ΔE_{ex} is the onsite exchange splitting. We have used $D_R \sim \frac{M}{\Delta E_{\text{ex}}}$, and $D_{RR'} \sim \frac{M}{\Delta E_{\text{ex}}} \times (\frac{2t}{\Delta E_{\text{ex}}})^2$.

Some additional comments. Our formalism here is not applicable to the non-magnetic systems, where $M(\mathbf{r}) = 0$ everywhere. Then we need to determine U in other ways. A possibility is utilizing the static numerical linear-response calculations; it gives the information of the static ($\omega = 0$) part of $\chi_{\mathbf{q}}^{+-}$ directly (easiest spin-polarization mode at each site). Then it will be possible to determine U from such informations together with some additional assumptions. In the case of systems like Gd where the d shell and f shell can polarize separately, we may need to extend our formulation so as to include non-locality of U (e.g. U can be parametrized as U_{ijkl} where i, j, k, l are atomic eigenfunction basis for d or f channel).

III. RESULT AND DISCUSSION

A. MnO and NiO

Fig. 1 shows the calculated SW energies $\omega(\mathbf{q})$ for MnO and NiO. (We used 1728 k -points in the BZ for all calculations, including MnAs.) $\omega(\mathbf{q})$ calculated from the LDA is too large, as earlier workers have found^{5,6}. The detailed shape of $\omega(\mathbf{q})$ is different from earlier work however: in Ref. 5, peaks in $\omega(\mathbf{q})$ occur near 200 meV for NiO, much lower than what we find. QSGW predicts $\omega(\mathbf{q})$ in good agreement with experimental data.

The difference of results between QSGW and LDA is understood by Eq. (16). $J_{RR'}$ between nearest AF sites essentially determine the SW energies (exactly speaking, three J parameters as shown in Table I). The LDA severely underestimates ΔE_{ex} . This can be corrected by LDA+ U , however, Solovyev and Terakura⁶ showed that it fails to reproduce SW energies as we mentioned in the introduction. This means that the transfer t is also wrong in LDA+ U ; in fact t is through the hybridization with Oxygen 2 p (superexchange). In other words, the agreements with SW experiments in QSGW indicates that both of them are well described by QSGW. Together with the fact that QSGW showed good agreements with optical experiments^{15,19} for MnO and NiO, we claim that our one-particle picture given by QSGW captures the essence of the physics for these systems. Our claim here is opposite to Refs.5,25 where they claimed that the one-particle picture can not capture the essence.

B. α -MnAs

Because α -MnAs is observed to be a FM with a moment of $3.4\mu_B$ ⁴⁴, we construct H^0 assuming a FM ground state. Inspection of the density of states (DOS) in Fig. 4, shows that QSGW predicts $\Delta E_{\text{ex}} \sim 1.0\text{ eV}$ larger the LDA. This difference is reflected in the spin moment: $M_a = 3.51\mu_B$ in QSGW, $3.02\mu_B$ in LDA. Fig. 2 shows the imaginary part of $\text{Tr}[\chi^{+-}(\mathbf{q}, \omega)]$ along $\Gamma - K$ line. Sharp SW peaks are seen at small \mathbf{q} ; they broaden with increasing \mathbf{q} . Fig. 3 shows the peak positions, corresponding to SW energies $\omega(\mathbf{q})$. Hatchmarks indicate the full-width at half-maximum, extracted from data such as that depicted in Fig. 2. This corresponds to the inverse lifetime of a SW which decays into spin-flip excitations. (Our calculation gives no width for MnO and NiO, because of the large gap for the spin-flip excitations). SW peaks are well identified all the way to the BZ boundary.

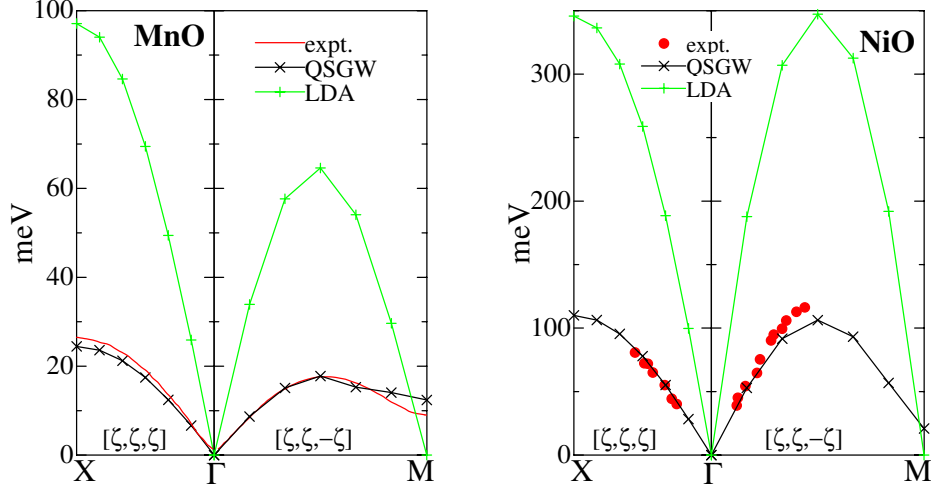


FIG. 1: (color online) Spin wave dispersion $\omega(\mathbf{q})$ for MnO and NiO calculated from the LDA and QSGW. Solid line without symbols in MnO or dots in NiO (red) are experimental values^{42,43}. We used experimental lattice constants 4.55 and 4.17 Å for MnO and NiO respectively.

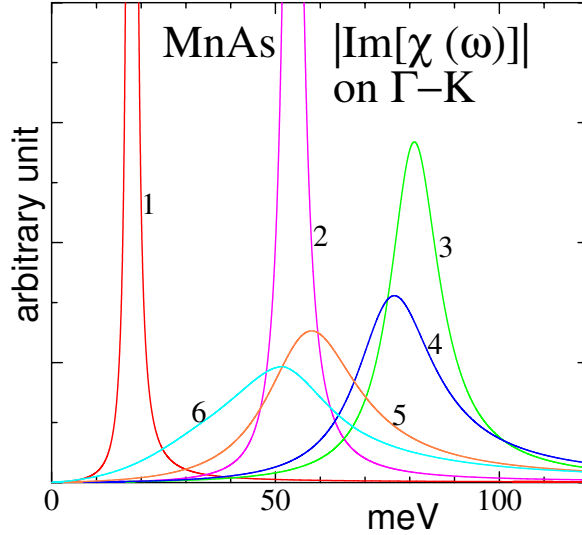


FIG. 2: (color online) Im part of $\text{Tr}[\chi^{+-}(\mathbf{k}, \omega)]$ for QSGW. Data are for 6 k -points, all along the Γ -K line. The k -point is $i/6$ K (thus $i=6$ falls at K). Peak positions and full-width-half-maxima are shown in the Γ -K line of Fig. 3.

We find that the collinear FM ground state is not stable in the LDA: as Fig. 3 shows, $\omega(\mathbf{q}) < 0$ around K. (Among all possible *collinear* configurations, the FM state may be the most stable. We did not succeed in finding any collinear configuration more stable than the FM one. A similar conclusion was drawn for the PBE GGA functional³¹.) On the other

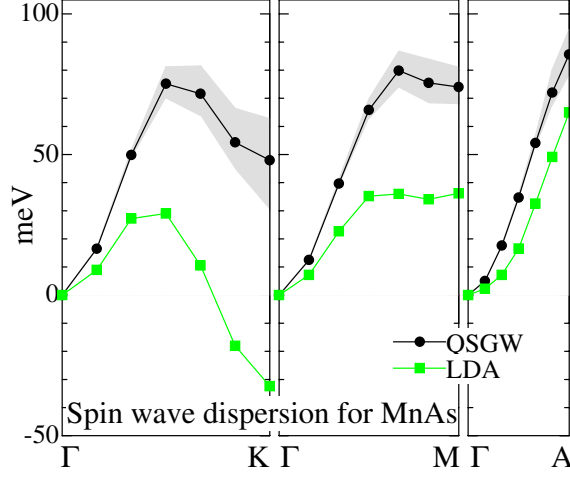


FIG. 3: (color online) Spin wave dispersion $\omega(\mathbf{q})$ in α -MnAs. QSGW results (circles) are enveloped by hatched regions, which indicate the full-width at half-maximum of the spin wave, and is a measure of the rate of SW decay. LDA (squares) predicts negative SW energies around K; indicating that the collinear FM ground state is not stable. The experimental lattice constants $a=3.70$ Å and $c/a=1.54$ were used.

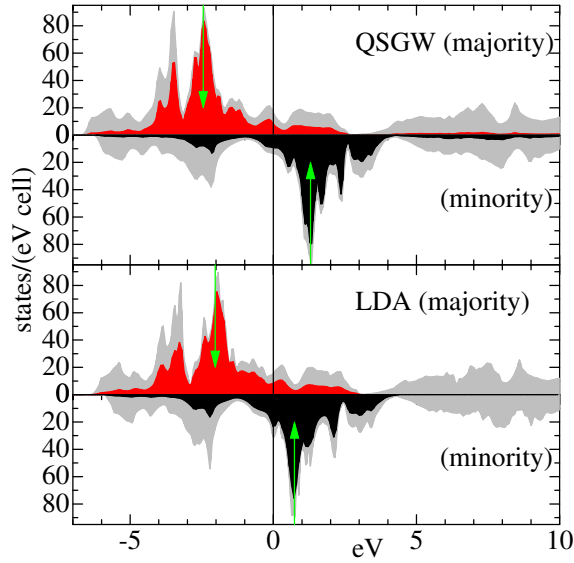


FIG. 4: (color online) quasiparticle DOS for α -MnAs. Lighter hatchings indicate total DOS; darker(black and red) hatchings indicate the partial d contribution, whose centers of gravity are shown by arrows. The Fermi energy is at zero.

hand, QSGW predicts stable collinear ground state, that is, $\omega(\mathbf{q}) > 0$ everywhere. However, even in QSGW, the SW energies are still low around K, which is a vector that connects nearest neighbor Mn sites in x-y plane. If this SW energy is further lowered for some reason, we may have a frustrated spin system because of the triangle (honeycomb) lattice of the Mn sites. This could be related to the anomalous phase diagram of MnAs, which can easily occur through the small changes in lattice structure associated with higher-temperature phases.

We can qualitatively understand the difference of SW energies between QSGW and LDA from the difference of ΔE_{ex} . Let us consider the energy difference of FM and AFM states for two-site model as illustrated in Ref.41. Then the energy gain of a FM pair is independent of ΔE_{ex} when some of majority states are occupied (less than half filling); we measure the energy from the majority spin's atomic level as the zero. In contrast, the gain of a AFM pair increases with decreasing ΔE_{ex} . Overall, the LDA with its smaller ΔE_{ex} , should contain a stronger AFM tendency.

C. Determined Parameters and related Quantities

Table I shows the effective interaction U_a^0 (interaction between unit spins). In NiO and MnO, U_a^0 as calculated by LDA is much smaller than the QSGW result. This is because the LDA underestimates bandgaps in NiO and MnO, thus overestimates the screening. U_a^0 is twice larger in NiO than in MnO. This is because $M_a(\mathbf{r})$ is more localized in NiO; in fact, the QSGW dielectric constants ϵ_∞ are similar ($\epsilon_\infty = 3.8(\text{MnO})$ and $4.3(\text{NiO})^{19}$), suggesting that the screened Coulomb interaction $U(\mathbf{r}, \mathbf{r}')$ is similar in the two materials. U_a^0 is smaller in MnAs than in MnO, because it is a metal.

For MnO and NiO, we confirmed that $J_{RR'}$ is non-negligible only for the three nearest-neighbors (NN) (Table I). J_{1+} and J_{1-} refer to 1st NN, spins parallel and spins antiparallel, respectively. J_2 refers to 2nd NN⁴². J_{1+} and J_{1-} by QSGW are quite different in MnO, while in LDA $J_{1+} \approx J_{1-}$, resulting in $\omega(\text{M}) \approx 0$ in that case.

For MnAs in QSGW, the expansion coefficients written as $(M^{-1})_{aa'} \equiv \frac{\partial(D^{\mathbf{q}\omega})_{aa'}^{-1}}{\partial\omega}|_{\omega=0}$, is rather dependent on \mathbf{q} ; nor is $(M^{-1})_{aa'} \propto \delta_{aa'}$. Off-diagonal contributions of $(M^{-1})_{aa'}$ give $\sim 10\%$ contribution to SW energies. In addition, its inverse of the diagonal element $1/(M^{-1})_{aa}$ is reduced by $\sim 0.5\mu_B$ at certain points in the BZ. In this case, mapping to a Heisenberg Hamiltonian has less clear physical meaning.

TABLE I: Magnetic parameters calculated by QSGW and LDA (in parenthesis). Muffin-tin radii R for cations were taken to be 2.48 (MnO), 2.33 (NiO), and 2.42 (MnAs) a.u. M_a is the spin moment within the muffin tin. Our approximation is equivalent to the assumption for U as $U(\mathbf{r}, \mathbf{r}', \omega) = \sum_a (U_a^0 + \omega U_a^1 + \dots) e_a(\mathbf{r}) e_a(\mathbf{r}')$ in Eq. (6). Then U_a^0 is written as $U_a^0 = \int_a d^3r \int_a d^3r' e_a(\mathbf{r}) e_a(\mathbf{r}') U(\mathbf{r}, \mathbf{r}', \omega = 0)$. Exchange parameters J_{1+}, J_{1-}, J_2 are shown for MnO and NiO. Total spin moments for MnAs are $7.00\mu_B/\text{cell}$ (QSGW) and $5.89\mu_B/\text{cell}$ (LDA). Our definition of J_{1+}, J_{1-}, J_2 follows that of Ref. 6, except we distinguish J_{1+} and J_{1-} ⁴².

	MnO	NiO	α -MnAs
U_a^0 (eV)	2.43 (0.95)	4.91 (1.64)	1.08 (0.93)
M_a (μ_B)	4.61 (4.35)	1.71 (1.21)	3.51 (3.02)
J_{1+} (meV)	-2.8 (-14.7)	-0.77 (0.3)	
J_{1-}	-4.8 (-14.7)	-1.00 (0.3)	
J_2	-4.7 (-20.5)	-14.7 (-28.3)	
T_N or T_c (K)	111	275	510
(experiment)	122 ^a	523 ^a	400

^aRef.⁴⁵

D. Calculation of T_N and T_c based on the Heisenberg model

From obtained $J_{RR'}$, we estimated T_N (T_c for MnAs) for QSGW (Table I) using the cluster variation method adapted to the Heisenberg model⁴⁶, which assumes classical dynamics of spins under \mathcal{H} . In NiO, the calculated T_N is only $\sim 50\%$ of experiment. There are two important effects that explain the discrepancy: (a) QSGW overestimates the dd exchange splitting^{17,19}, and (b) the classical treatment of quantum dynamics of spins under \mathcal{H} . Both effects will increase T_N . Considering that QSGW well reproduces SW energies (Fig. 1), the errors connected with (a) would not seem to be so serious in MnO and NiO. (b) can be rather important, especially when the local moment is small. This is a general problem as discussed in Ref. 5: Heisenberg parameters that reproduce SW energies well in NiO do not yield a correspondingly good T_N . If we multiply our classical T_N by a factor $S(S+1)/S^2 \approx 1.86$ (as $2S = M_a = 1.71$), which is the ratio of quantum to classical T_N in mean field theory, we have better agreement with experiment. This is what Hutchings et al. used⁴³. On the other

hand, evaluation of the quantum Heisenberg model using a Green's function technique show that the mean-field theory rather strongly overestimates quantum corrections⁴⁷. Also, T_N is already close to the experimental value in MnO. This is explained in part because correction (b) is less important in MnO, since S is larger. Further, we have large contributions to T_N from $J_{1\pm}$ in MnO, but not in NiO. Around T_N , J_{1+} and J_{1-} will tend to approach some average value, which reduces $\omega(\mathbf{q})$ and therefore T_N (recall $\omega(\mathbf{M})=0$ when $J_{1+}=J_{1-}$). The temperature-dependence of J is not accounted for here.

$J_{RR'}$ exhibits long-ranged, oscillatory behavior in MnAs: its envelope falls off as $|\mathbf{R}-\mathbf{R}'|^3$ as predicted by RKKY theory for a metal. Consequently, it is not so meaningful to estimate T_c from just a few NN, as was done recently^{31,32}. Shells up to 25th-neighbors are required to converge T_c to within 5% or so. The calculated T_c is 110K too high in comparison with experiment. Taking (a) into account will improve the agreement; however, there are many factors that make a precise calculation very difficult. We also need to take (b) into account; in addition, other factors such as assumptions within the Heisenberg model, may give non-negligible contributions.

In conclusion, we present a simple method to calculate spin susceptibility, and applied it in the QSGW method. SW energies for MnO and NiO are in good agreement with experiments; in α -MnAs the FM ground state is stable, which also agrees with experiment (to our knowledge, no SW energies have been published in α -MnAs). LDA results come out very differently in each material. By mapping to the Heisenberg model, we estimated T_N or T_c . We found some disagreement with experiments, and discussed some possible explanations.

Acknowledgments

We thank M. I. Katsnelson, W.R.Lambrecht, and V.P. Antropov for valuable discussions. This work was supported by DOE contract DE-FG02-06ER46302. We are also indebted to the Ira A. Fulton High Performance Computing Initiative.

APPENDIX A: STATIC $J(q)$ CALCULATION— HEISENBERG MODEL

We derive the linear response to an external magnetic field \mathbf{B} for the Heisenberg model, whose Hamiltonian is given as

$$\mathcal{H} = - \sum_{\mathbf{T}a} \sum_{\mathbf{T}'a'} J_{\mathbf{T}a\mathbf{T}'a'} \mathbf{S}_{\mathbf{T}a} \cdot \mathbf{S}_{\mathbf{T}'a'} + g\mu_B \sum_{\mathbf{T}a} \mathbf{S}_{\mathbf{T}a} \cdot \mathbf{B}_{\mathbf{T}a}, \quad (\text{A1})$$

where $\mathbf{S}_{\mathbf{T}a}$ is the spin at $\mathbf{T}a$ (\mathbf{T} is for primitive cell, a specify magnetic site in a cell). $J_{\mathbf{T}a\mathbf{T}a} = 0$. $J_{\mathbf{T}a\mathbf{T}'a'} = J_{\mathbf{T}'a'\mathbf{T}a}$. The equation of motion $-i\hbar\dot{\mathbf{S}}_{\mathbf{T}a} = [\mathcal{H}, \mathbf{S}_{\mathbf{T}a}]$ is written as

$$\hbar\dot{\mathbf{S}}_{\mathbf{T}a} = \mathbf{S}_{\mathbf{T}a} \times \left(2 \sum_{\mathbf{T}'a'} J_{\mathbf{T}a\mathbf{T}'a'} \mathbf{S}_{\mathbf{T}'a'} - g\mu_B \mathbf{B}_{\mathbf{T}a} \right) \quad (\text{A2})$$

We introduce $g\mu_B \mathbf{B} = 2\mathbf{b}$, and $\mathbf{S}_{\mathbf{T}a} = \mathbf{S}_{\mathbf{T}a}^0 + \Delta\mathbf{S}_{\mathbf{T}a}$. $\mathbf{S}_{\mathbf{T}a}^0$ is the static spin configuration. Then Eq. (A2) reduces to

$$\begin{aligned} \hbar\dot{\Delta\mathbf{S}}_{\mathbf{T}a} &= \mathbf{S}_{\mathbf{T}a}^0 \times \left(2 \sum_{\mathbf{T}'a'} J_{\mathbf{T}a\mathbf{T}'a'} \Delta\mathbf{S}_{\mathbf{T}'a'} \right) + \Delta\mathbf{S}_{\mathbf{T}a} \times \left(2 \sum_{\mathbf{T}'a'} J_{\mathbf{T}a\mathbf{T}'a'} \mathbf{S}_{\mathbf{T}'a'} \right) - 2\mathbf{S}_{\mathbf{T}a}^0 \times \mathbf{b}_{\mathbf{T}a} \\ &= \sum_{\mathbf{T}'a'} \left(2\mathbf{S}_{\mathbf{T}a}^0 J_{\mathbf{T}a\mathbf{T}'a'} \right) \times \Delta\mathbf{S}_{\mathbf{T}'a'} - \left(2 \sum_{\mathbf{T}'a'} J_{\mathbf{T}a\mathbf{T}'a'} \mathbf{S}_{\mathbf{T}'a'}^0 \right) \times \Delta\mathbf{S}_{\mathbf{T}a} - 2\mathbf{S}_{\mathbf{T}a}^0 \times \mathbf{b}_{\mathbf{T}a} \end{aligned} \quad (\text{A3})$$

Introducing the Fourier transform, $\Delta\mathbf{S}_{\mathbf{T}a} = \frac{1}{N} \sum_{\mathbf{k}} \Delta\mathbf{S}_a(\mathbf{k}) e^{i\mathbf{k}(\mathbf{T}+\mathbf{a})}$, Eq. (A3) reduces to

$$\hbar\dot{\Delta\mathbf{S}}_a(\mathbf{k}) = \sum_{a'} \left(2\mathbf{S}_a^0 J_{aa'}(\mathbf{k}) - \left(2 \sum_{a''} J_{aa''}(0) \mathbf{S}_{a''}^0 \right) \delta_{aa'} \right) \times \Delta\mathbf{S}_{a'}(\mathbf{k}) - 2\mathbf{S}_a^0 \times \mathbf{b}_a(\mathbf{k}). \quad (\text{A4})$$

Assuming $\Delta\mathbf{S}_a(\mathbf{k}) \propto e^{-i\omega t/\hbar}$, we have

$$\sum_{a'} \left(\frac{i\omega\delta_{aa'}}{2} + \mathbf{S}_a^0 J_{aa'}(\mathbf{k}) - \left(\sum_{a''} J_{aa''}(0) \mathbf{S}_{a''}^0 \right) \delta_{aa'} \right) \times \Delta\mathbf{S}_{a'}(\mathbf{k}) = \mathbf{S}_a^0 \times \mathbf{b}_a(\mathbf{k}). \quad (\text{A5})$$

Let us consider the collinear ground state. Then $\mathbf{S}_a^0 = S_a \mathbf{e}_z$ (S_a is the size of spin, including sign). We have

$$\sum_{a'} \left(\frac{i\omega\delta_{aa'}}{2S_a} \right) \Delta\mathbf{S}_{a'}(\mathbf{k}) + \sum_{a'} \left(J_{aa'}(\mathbf{k}) - \left(\sum_{a''} \frac{1}{S_a} J_{aa''}(0) S_{a''} \right) \delta_{aa'} \right) \mathbf{e}_z \times \Delta\mathbf{S}_{a'}(\mathbf{k}) = \mathbf{e}_z \times \mathbf{b}_a(\mathbf{k}) \quad (\text{A6})$$

Using $\mathbf{S} = S^+ \frac{\mathbf{e}_x - i\mathbf{e}_y}{2} + S^- \frac{\mathbf{e}_x + i\mathbf{e}_y}{2} + S^z \mathbf{e}_z$, and $\mathbf{e}_z \times (\mathbf{e}_x \pm i\mathbf{e}_y) = \mp i(\mathbf{e}_x \pm i\mathbf{e}_y)$ we have,

$$\sum_{a'} \left(\frac{\omega\delta_{aa'}}{2S_a} - \bar{J}_{aa'}(\mathbf{k}) \right) S_{a'}^+(\mathbf{k}) = b_a^+(\mathbf{k}). \quad (\text{A7})$$

$$\sum_{a'} \left(\frac{\omega\delta_{aa'}}{2S_a} + \bar{J}_{aa'}(\mathbf{k}) \right) S_{a'}^-(\mathbf{k}) = b_a^-(\mathbf{k}), \quad (\text{A8})$$

where

$$\bar{J}_{aa'}(\mathbf{k}) = J_{aa'}(\mathbf{k}) - \left(\sum_{a''} \frac{1}{S_a} J_{aa''}(0) S_{a''} \right) \delta_{aa'} \quad (\text{A9})$$

Only the difference between $\bar{J}_{aa'}(\mathbf{k})$ and $J_{aa'}(\mathbf{k})$ are diagonal parts. These are determined so that $\int d^3k J_{aa}(\mathbf{k}) = 0$. Eq. (A7) is the same as Eq. (14).

-
- ¹ T. Moriya, Y. Takahashi, and K. Ueda, Journal of the Physical Society of Japan **59**, 2905 (1990), 39.
 - ² A. J. Millis, H. Monien, and D. Pines, Physical Review B **42**, 167 (1990), 30 Part A.
 - ³ G. G. Lonzarich and L. Taillefer, J. Phys. C: Solid State Phys. **18**, 4339 (1985).
 - ⁴ S. N. Kaul, J. Phys: Cond. Matter **11**, 7597 (1999).
 - ⁵ X. Wan, Q. Yin, and S. Y. Savrasov, Phys. Rev. Lett. **97**, 266403 (2006).
 - ⁶ I. V. Solov'yev and K. Terakura, Phys. Rev. B **58**, 15496 (1998).
 - ⁷ T. Kotani, J.Phys.: Condens. Matter **10**, 9241 (1998).
 - ⁸ J. Muscat, A. Wander, and N. M. Harrison, Chemical Physics Letters **342**, 397 (2001), 33.
 - ⁹ A. D. Becke, The Journal of Chemical Physics **98**, 5648 (1993).
 - ¹⁰ C. Franchini, V. Bayer, R. Podloucky, J. Paier, and G. Kresse, Phys. Rev. B **72**, 045132 (2005).
 - ¹¹ J. P. Perdew, K. Burke, and M. Ernzerhof, Phys. Rev. Lett. **77**, 3865 (1996).
 - ¹² I. de P. R. Moreira, F. Illas, and R. L. Martin, Phys. Rev. B **65**, 155102 (2002).
 - ¹³ F. Fuchs, J. Furthmüller, F. Bechstedt, M. Shishkin, and G. Kresse, Physical Review B **76**, 115109 (2007).
 - ¹⁴ J. Paier, M. Marsman, and G. Kresse, The Journal of Chemical Physics **127**, 024103 (2007).
 - ¹⁵ S. V. Faleev, M. van Schilfgaarde, and T. Kotani, Phys. Rev. Lett. **93**, 126406 (2004).
 - ¹⁶ A. N. Chantis, M. van Schilfgaarde, and T. Kotani, Phys. Rev. Lett. **96**, 086405 (2006).
 - ¹⁷ M. van Schilfgaarde, T. Kotani, and S. Faleev, Phys. Rev. Lett. **96**, 226402 (2006).
 - ¹⁸ A. N. Chantis, M. van Schilfgaarde, and T. Kotani, Physical Review B **76**, 165126 (2007).
 - ¹⁹ T. Kotani, M. van Schilfgaarde, and S. V. Faleev, Physical Review B **76**, 165106 (pages 24) (2007).
 - ²⁰ F. Bruneval, N. Vast, L. Reining, M. Izquierdo, F. Sirotti, and N. Barrett, Physical Review Letters **97**, 267601 (2006).

- ²¹ M. Shishkin, M. Marsman, and G. Kresse, Physical Review Letters **99**, 246403 (2007).
- ²² F. Sottile, V. Olevano, and L. Reining, Phys. Rev. Lett. **91**, 056402 (2003).
- ²³ K. Terakura, A. R. Williams, T. Oguchi, and J. Kübler, Phys. Rev. Lett. **52**, 1830 (1984).
- ²⁴ M. Tanaka *et al*, Jour. Vac. Sci. Tech. B **12**, 1091 (1994).
- ²⁵ J. Kunes, V. I. Anisimov, S. L. Skornyakov, A. V. Lukoyanov, and D. Vollhardt, Physical Review Letters **99**, 156404 (2007).
- ²⁶ A. G. Petukhov, I. I. Mazin, L. Chioncel, and A. I. Liechtenstein, Phys. Rev. B **67**, 153106 (2003).
- ²⁷ J. H. Shim, K. Haule, and G. Kotliar, NATURE **446** (2007).
- ²⁸ A. Fujimori and F. Minami, Phys. Rev. B **30**, 957 (1984).
- ²⁹ H. Akai and P. H. Dederichs, Phys. Rev. B **47**, 8739 (1993).
- ³⁰ J. W. D. Connolly and A. R. Williams, Phys. Rev. B **27**, 5169 (1983).
- ³¹ I. Rungger and S. Sanvito, Phys. Rev. B **74**, 024429 (2006).
- ³² L. M. Sandratskii and E. Sasioglu, Phys. Rev B **74**, 214422 (2006).
- ³³ T. Oguchi, K. Terakura, and A. R. Williams, Phys. Rev. B **28**, 6443 (1983).
- ³⁴ A. I. Liechtenstein, M. I. Katsnelson, V. P. Antropov, and V. A. Gubanov, J. Magn. Magn. Mater. **67**, 65 (1987).
- ³⁵ J. F. Cooke, J. W. Lynn, and H. L. Davis, Phys. Rev. B **21**, 4118 (1980).
- ³⁶ S. Y. Savrasov, Phys. Rev. Lett. **81**, 2570 (1998).
- ³⁷ K. Karlsson and F. Aryasetiawan, Phys. Rev. B **62**, 3006 (2000).
- ³⁸ V. P. Antropov, J. Mag. Mag. Mat. **262**, L192 (2003).
- ³⁹ M. I. Katsnelson and A. I. Lichtenstein, Journal of Physics-Condensed Matter **16**, 7439 (2004).
- ⁴⁰ P. W. Anderson and H. Hasegawa, Phys. Rev. **100**, 675 (1955).
- ⁴¹ M. v. Schilfhaarde and O. N. Mryasov, Phys. Rev. B **63**, 233205 (2001).
- ⁴² Y. Kohgi, I. Ishikawa, and Y. Endoh, Solid State Communication **11**, 391 (1972).
- ⁴³ M. T. Hutchings and E. J. Samuelsen, Phys. Rev. B **6**, 3447 (1972).
- ⁴⁴ J. B. Goodenough and J. A. Kafalas, Phys. Rev. **157**, 389 (1967).
- ⁴⁵ W. L. Roth, Phys. Rev. **110**, 1333 (1958).
- ⁴⁶ J. L. Xu, M. van Schilfhaarde, and G. D. Samolyuk, Phys. Rev. Lett. **94**, 097201 (2005).
- ⁴⁷ R. Y. Gu and V. P. Antropov, preprint <http://arxiv.org/abs/cond-mat/0508781>.